JOURNAL OF MATERIALS SCIENCE 31 (1996) 3763–3768

Microstructure and properties of a RS/PM Al–Fe–Co alloy

V. STEFÁNIAY, A. LENDVAI*, T. TURMEZEY
ALUTERV-FKI Ltd., HUNGALU Engineering and Development Centre, H-1502, Budapest, P.O.B. 308, Hungary

The extruded Al–8%Fe–2%Co RS/PM alloy, produced by gas atomization, exhibited UTS = 460 MPa and 8% elongation at room temperature, and UTS = 250 MPa at 300 °C. The properties are strongly influenced by the powder microstructure and the processing conditions used. The optimum mechanical properties can be obtained by the use of powder fraction with particle size < 63 μm. A temperature of about 400 °C proved to be the best compromise for degassing and extrusion in order to achieve a low hydrogen content without considerable dispersoid coarsening.

1. Introduction

One group of elevated temperature powder metallurgical (PM) alloys produced by a rapid solidification (RS) technique was developed on Al–Fe base containing a eutectic with other transition elements such as Mn, Ni and Co or a rare earth element such as Ce [1]. In these types of alloys fine intermetallic compounds, which give strength, form in a substantial volume fraction during solidification [2–8]. These strengthening dispersoids which yield the good elevated temperature properties of these RS/PM alloys tend to coarsen above 300 °C. The initial size distribution of the strengthening particles is largely influenced by the solidification rate of the metal during the gas atomization process, while the particle coarsening and therefore the elevated temperature properties depend on further processing (degassing, extrusion, etc.) of the alloy powder.

A RS/PM Al–Fe–Co alloy produced by gas atomization was investigated in order to determine the effects of processing conditions on the microstructure of the powder and microstructure and mechanical properties of the extruded alloy.

2. Experimental details

The aluminium-rich Al–Fe–Co alloy was produced on a 99.99% pure Al base by argon gas atomization at ALUTERV-FKI Ltd. The alloy with 5% Fe and 2% Co nominal composition has a real composition of 7.6% Fe and 1.7% Co according to its chemical analysis. The alloy powder was screened and investigated for three different particle size fractions: < 63, 63 – 90 and 90 – 200 μm. The Al–Fe–Co powder was further processed by cold isostatic pressing (CIP), vacuum degassing and hot extrusion. The alloy powder was compacted by CIP to a density of about 75% using a pressure of 200 MPa. Degassing was carried out in vacuum ($\sim 10^{-2}$ Pa) at 400 °C for 1 h. The degassed and compacted samples were extruded into bars with a diameter of 5 to 8 mm at 400 °C with an extrusion ratio, $\lambda = 10$ to 36.

The morphology and the structure of the powder and extruded alloy were investigated by scanning (SEM) and transmission (TEM) electron microscopy. Phase analysis was carried out by X-ray diffraction (XRD) method. The process of degassing in the cold compacted material was followed by thermal analysis together with quadrupole mass spectrometric analysis. Hydrogen content was determined by a hydrogen gas analyser of ITHAC (Adainel-Lhomargy) type. Mechanical properties of the extruded alloy were characterized by Brinell hardness and tensile measurements carried out in the longitudinal direction of the extruded samples.

3. Results and discussion

3.1. Characteristics of alloy powder

The argon atomized powder particles are of typical spheroid morphology. On the SEM micrograph (Fig. 1) a particle with an inhomogeneous microstructure taken from the powder fraction of less than 63 μm in particle size can be seen. The solidification within a particle can start from one or more nuclei. During solidification its velocity slows down because of recalescence resulting in a coarser microstructure than that of the first solidified part of the particles [9–11]. The microstructural inhomogeneity of the powder could also be observed on a finer scale by TEM. Powder particles with very different microstructures can be seen. Inside a powder particle there is a typical coupled eutectic structure in one of the grains and a finer or coarser dendritic structure in the other ones (Fig. 2). A similar coupled eutectic can also form in the

* *Present address*: SEMILAB Semiconductor Physics Laboratory Ltd., H/1047, Budapest, Fóti út 56., Hungary.

0022–2461

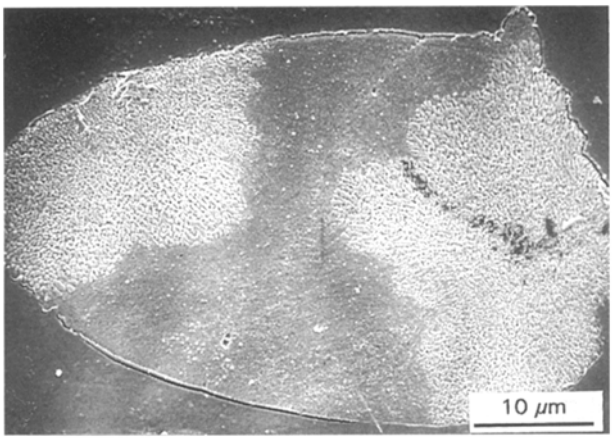

Figure 1 SEM micrograph of a powder particle.

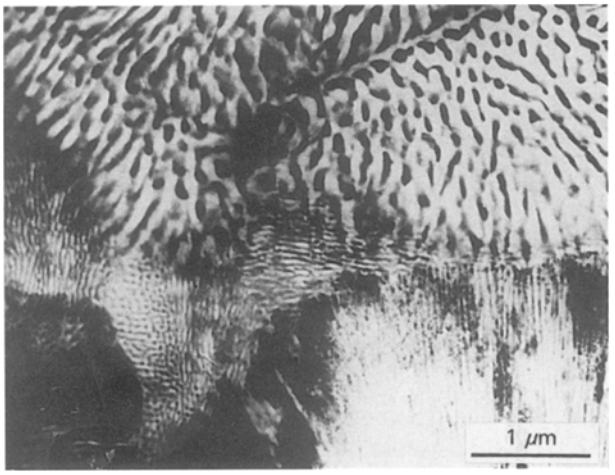

Figure 2 TEM micrograph of the powder alloy.

rapidly solidified hypereutectic Al–Fe–Ni powder alloy [4, 5].

The degree of microstructural inhomogeneity in the atomized powder with particle size over a wide range can be reduced by screening the powder to obtain a relatively narrow size range. However the microstructural inhomogeneity cannot be completely diminished by any subsequent procedure [11]. The nonuniformity of the microstructure of the powders results in inhomogeneities in the extruded material. In the as-atomized alloy powder, with size between 90 and 200 μm, the $Al_9(CoFe)_2$ metastable ternary intermetallic compound is found using XRD. The intermetallic compounds are situated in the interdendritic region as can be seen in Fig. 2. During a heat treatment at 500 °C for 24 h it mainly transforms into the stable $Al_3(Fe, Co)$.

3.2. Strengthening particles and their stability in the extruded alloy

In the extruded material, intermetallic phases of globular shape can be found (Fig. 3), which are located at the grain boundaries and inside the grains as well. These $Al_9(CoFe)_2$ intermetallic compounds determined by XRD probably act as strengthening particles in this alloy.

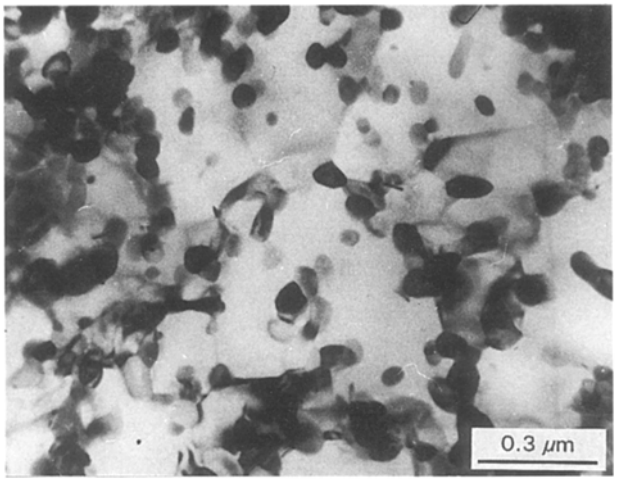

Figure 3 TEM micrograph of the extruded PM alloy.

TABLE I Ultimate tensile strength and hardness for extruded alloys made from powders with different particle size ($\lambda = 10$, degassed samples)

Powder fraction (μm)	Ultimate strength (MPa)			Macrohardness at $T = 20$ °C (HB)
	Test temperature (°C)			
	20	300	400	
< 63	460	250	62	124
63–90	424	243	67	129
90–200	315	192	101	87

There is a direct relationship between the hardness and strength of the extruded material and the powder particle size (Table I).

About a 30% increase in hardness and strength at room temperature can be attained if the powder material with particle size between 63 and 90 μm is used instead of one with a size between 90 and 200 μm. This difference in the strength of the extruded material made with powders of different particle sizes, decreases at a higher temperature as seen in elevated tensile testing. The smaller the powder particles are, the finer are the dispersoids which form during rapid solidification and therefore the more effective is their strengthening effect. Powder particles with a size of about 10 μm remained undeformed in the extruded alloy (Fig. 4d) which proves its higher hardness being resistant even to hot working.

After heat treatment at different temperatures for 100 h, coarsening of these dispersoids was observed by SEM investigations (Fig. 4a–d). The size and distribution of the intermetallic particles remain unchanged up to 300 °C, while a rapid coarsening of the dispersoids takes place at higher temperatures. The decreasing hardness and strength of the alloy at 300 °C (Table II) can be related to the particle coarsening.

Not only coarsening but phase transformation also occurs during annealing. Although the metastable $Al_9(CoFe)_2$ intermetallic compound formed in the powder does not transform during hot extrusion, it does transform completely into $Al_3(Fe, Co)$ in the

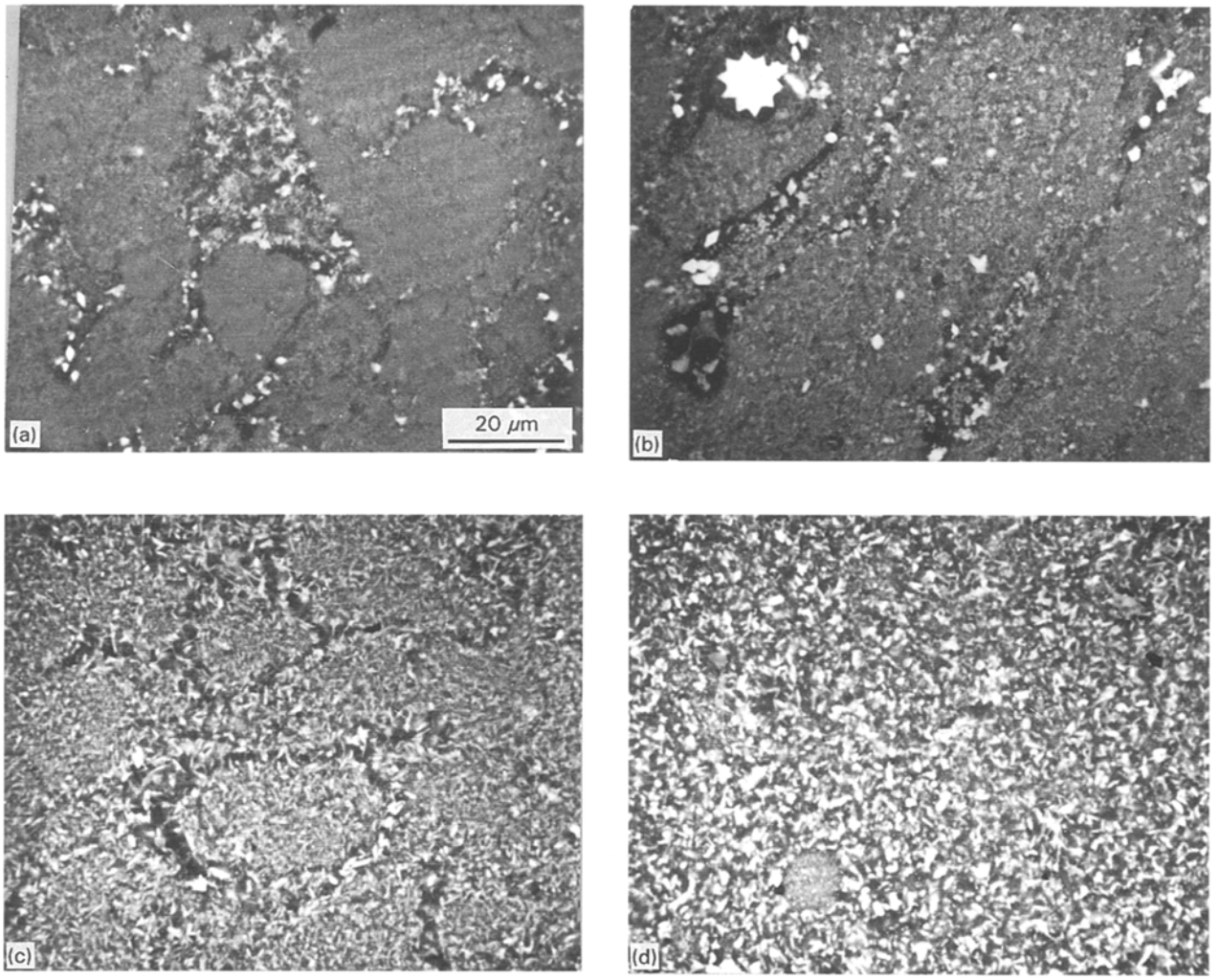

Figure 4 The effect of heat treatment on the structure of the extruded alloy. $t = 100$ h, (a) $T = 200\,°C$; (b) $T = 300\,°C$, (c) $T = 400\,°C$ and (d) $T = 500\,°C$ (SEM-BEI micrographs, same magnification).

TABLE II The effect of heat treatment ($t = 100$ h) on the ultimate strength, hardness and the electrical resistivity of the extruded alloy, (powder particle size 63–90 μm, $\lambda = 25$, degassed samples)

Temperature (°C)	R_m (MPa)	HB	ρ(Ω cm)
20	430	129	1.05
100	405	128	1.01
200	404	129	0.96
300	380	120	0.85
400	320	95	0.62
500	250	76	0.55

extruded alloy during a heat treatment at 500 °C for 24 h. Electrical resistivity measurements carried out on the heat treated alloys show that the solid solution content of the Al matrix decreased slightly up to 300 °C (Table II). At 300 °C first a slow reduction in electrical resistivity begins followed by a faster reduction as temperature increases. Three processes, namely precipitation, phase growth and phase transformation could take place at the same time during heat treatment above 300 °C, which together result in the rapid decrease of the resultant electrical resistivity.

TABLE III The influence of extrusion ratio (λ) on the hardness

Extrusion ratio, λ	HB
10	124
25	130
36	101

3.3. Relations between microstructure, processing and properties

The properties of extruded RS materials are influenced not only by the microstructure of the alloy powder, but by the processing conditions as well. Macrohardness of the extruded material is a function of extrusion ratio (λ) as shown in Table III. (Powder fraction < 63 μm.)

While the hardness remains unchanged between $\lambda = 10$ and 25, some decrease in its value can be observed at $\lambda = 36$. This decrease of the hardness can be due to the intensive heating of the material during the extrusion process with the higher extrusion ratio, which causes the coarsening of the strengthening particles.

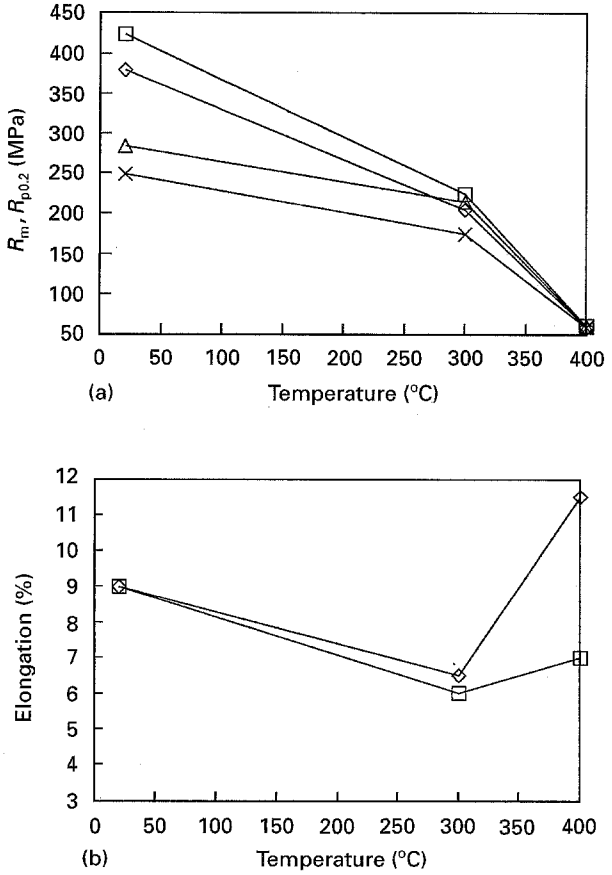

Figure 5 The influence of the degassing conditions on the elevated temperature tensile properties of the extruded alloy: (a) yield stress, tensile strength and (b) elongation. Key: (a) —◇— R_m (degassed), —□— R_m (without degassing), —×— R_p (degassed), —△— R_p (without degassing); (b) —◇— degassed, —□— without degassing.

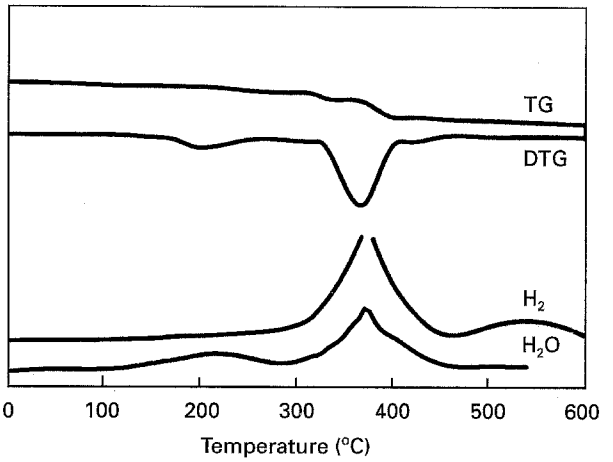

Figure 6 Degassing process of cold compacted alloy powder according to thermal and mass spectrometric analysis. TG = the change of mass by thermogravimetric analysis, DTG = the rate of mass change by differential thermogravimetric analysis.

The ultimate tensile strength (UTS) of the alloy tested at 300 °C is reduced by 30% as compared to that tested at room temperature (Table I). Tensile properties versus test temperature are compared for samples with and without degassing in Fig. 5a and b. The alloy without degassing has a higher initial UTS and yield strength (YS) than that with degassing. However the difference in properties diminishes when tested at 400 °C.

Tensile elongation decreases initially for both alloys and increases again as the test temperature is raised up to 400 °C. The minimum ductility at about 300 °C can be explained by the dynamic strain ageing (DSA) assumed by Skinner and co-workers [12]. The presence of dissolved atoms was proved by electrical resistivity (Table II). The precipitation of the solute atoms present in the extruded material takes place at and above 400 °C. This precipitation process explains the increase in ductility during the test at 400 °C. The role of the gas content appears only at this temperature because the increase in elongation is greater for the alloy prepared by degassing during PM processing. This is in good agreement with the results of Kim [6] for Al–Fe–Ce alloy.

All of these prove the importance of the degassing conditions. Although the strength of the material degassed at high temperature mostly reduces, its ductile property can be improved by this process. As described earlier [6], this is in connection with the hydrogen content. The hydrogen content of the extruded Al–Fe–Co alloy investigated was determined as 3.7 p.p.m. without degassing and 1.5 p.p.m. with it. The process of degassing was followed by thermal analysis with continuous heating. It begins with a mass decrease between 100 and 300 °C which is related to the evaporation of physisorbed H_2O detected by mass spectrometry (Fig. 6). The mass decrease between ~325 and 410 °C is caused by the desorption of H_2 and H_2O together. They are the volatile products of decomposing hydroxides from the surface oxide layer. Between 400 and 550 °C the dominant process is the desorption of H_2. In order to achieve a minimum H_2 content in the material, a degassing temperature above 500 °C would be preferable, as was also found by Kim *et al.* [10]. Degassing at such a high temperature, however, is detrimental to mechanical properties affected by dispersoid coarsening in this alloy. In practice degassing is carried out at a lower temperature of 350 or 400 °C. In this case dehydration of hydroxides in the surface oxide layer is not yet complete, and it has the form of $Al_2O_3 \cdot XH_2O$ ($0 < X < 1$), which still contains a certain amount of residual hydrogen. During elevated temperature tensile testing the oxide break-ups in the extruded material and may generate hydrogen which creates voids (Fig. 7). These voids can be seen in the vicinity of the fracture surface tested at different temperatures and their number increases with testing temperature. The number and the distribution of these voids are consistent with the morphology of the fracture surface of the tensile tested samples (Fig. 8).

The fracture surface of the alloy tested at 20 °C has a dimpled structure (Fig. 8a). The dimples are very small (0.5–3 μm). Although the formation of these dimples is initiated by the coalescence of voids, they cannot be seen in the longitudinal microstructure (Fig. 7a) because of their small size. The voids in the alloy tested at 400 °C are distributed along the powder grain boundaries in the extruded material (Fig. 7c). In

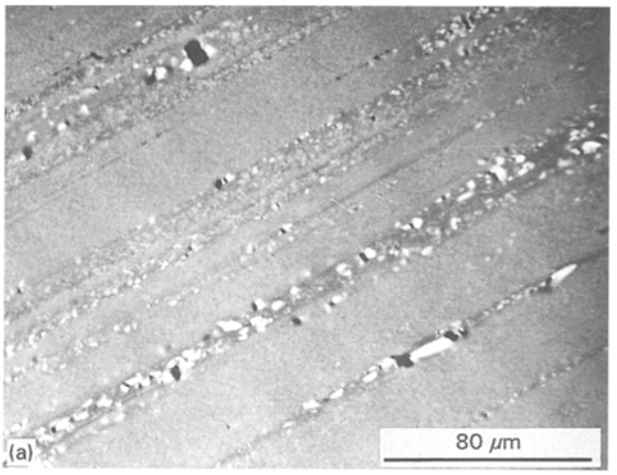

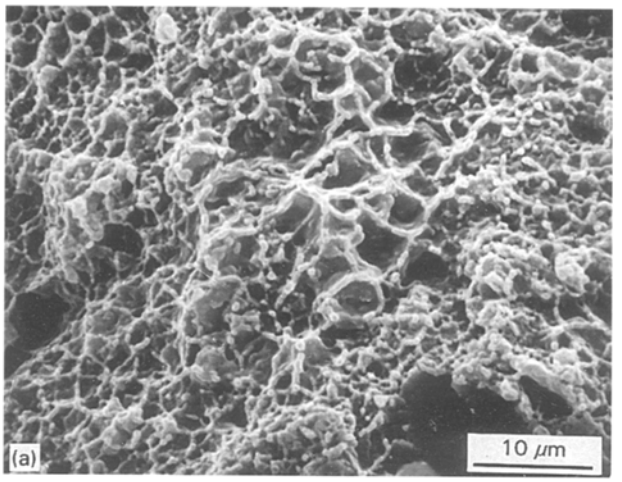

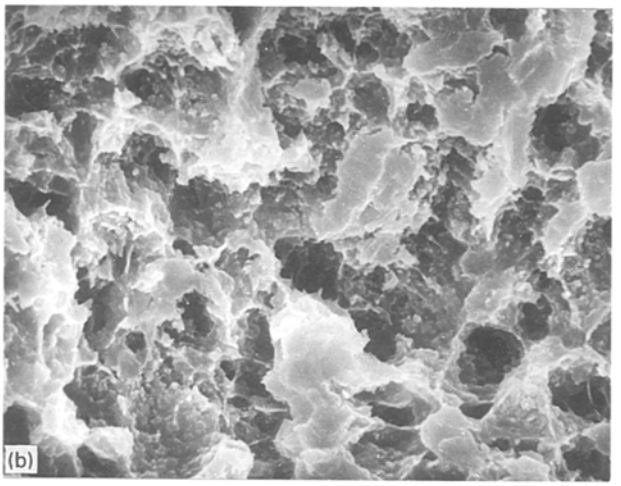

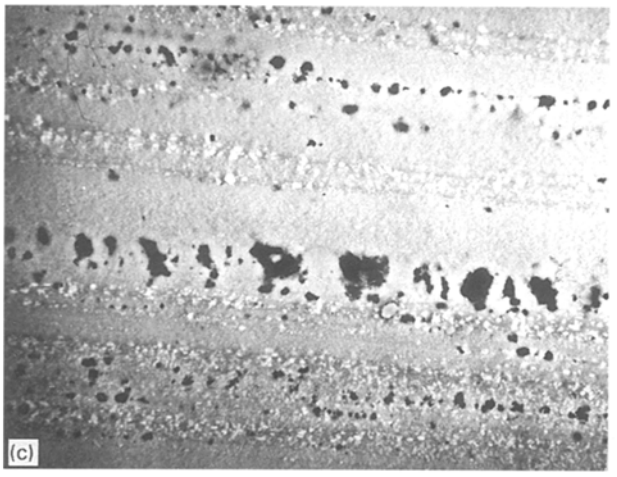

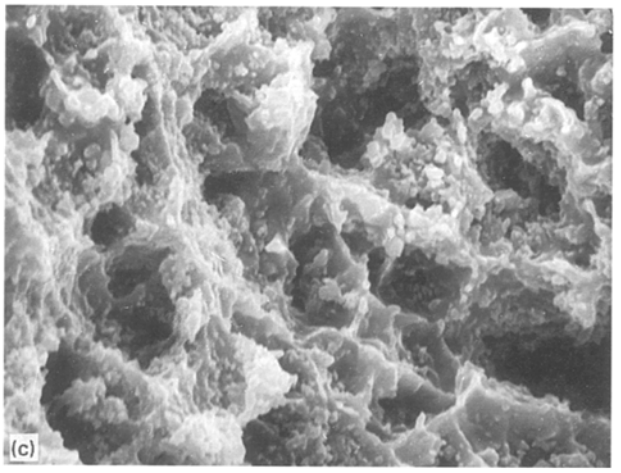

Figure 7 The longitudinal microstructure of the tensile tested samples. Test temperatures: (a) $T = 20\,^{\circ}C$, (b) $T = 300\,^{\circ}C$ and (c) $T = 400\,^{\circ}C$ (SEM-BEI micrographs, same magnification).

Figure 8 Tensile fracture surfaces of the alloys tested at (a) $T = 20\,^{\circ}C$; (b) $T = 300\,^{\circ}C$ and (c) $T = 400\,^{\circ}C$ (SEM micrographs, same magnification).

accordance with this void distribution the fracture surface of this alloy has an intergranular characteristic (Fig. 8c). Cracks can be observed in the transverse direction besides the voids (Fig. 7b) in the material tested at 300 °C exhibiting the least elongation. The appearance of cracks which can be seen as cleavage in the same part of the fracture surface (Fig. 8b) proves that the low ductility is not caused by the H_2 content but that the DSA may be responsible for this.

4. Conclusions

The extruded material made from AlFe8Co2 alloy powder, produced by gas atomization with powder sizes up to 200 μm, exhibits good mechanical properties at elevated temperature. UTS = 460 MPa and elongation 8% at room temperature and UTS = 250 MPa at 300 °C, which makes it suitable for high temperature applications. The properties are strongly influenced by the powder microstructure and

the processing conditions used. Hardness can be improved by the application of a smaller particle size. If the alloy is extruded with an extrusion ratio greater than 25, or the extruded alloy is heated above 300 °C, its room temperature hardness and strength are degraded. Both processes are caused by the coarsening of strengthening phases in the alloy. The parallel decrease of strength and ductility determined at elevated temperatures supports the operation of other mechanisms as well. It can be assumed that DSA caused by the interactions of solute atoms and dislocations is responsible for this effect.

Up to 300 °C the degassing has only a slight effect on the properties: it caused a small decrease in ultimate tensile strength while a small increase in elongation could be observed. At 400 °C, however degassing has no further effect on tensile strength but a considerable increase in elongation could be achieved by desorbing H_2 from the material.

Acknowledgement

This work was sponsored by the National Research Foundation (OTKA), contract Nr. 278.

References

1. F. H. FROES, Y.-W. KIM and S. KRISHNAMURTHY, *Mater. Sci. Eng.* **A117** (1989) 19.
2. M. A. ZAIDI and T. SHEPPARD, *Mater. Sci. Technol.* **3** (1987) 146.
3. M. A. ZAIDI, J. S. ROBINSON and T. SHEPPARD, *ibid.* **1** (1985) 737.
4. Y.-W. KIM and W. M. GRIFFITH, in "Rapidly Solidified Powder Aluminum Alloys", ASTM STP 890, edited by M. E. Fine and E. A. Starke, Jr. (American Society for Testing Materials, Philadelphia, 1986) pp. 485–511.
5. Y.-W. KIM and A. G. JACKSON, *Scripta Metall.* **20** (1986) 777.
6. Y.-W. KIM, in Proceedings of the Symposium on "Dispersion Strengthened Aluminium Alloys", Phoenix, Arizona, 1988, edited by Y.-W. Kim, W. M. Griffith, The Minerals, Metals and Materials Society, 1988, pp. 157–180.
7. *Idem, Progress Powder Metall.* **43** (1987) 13.
8. T. TURMEZEY and STEFÁNIAY, *Key Eng. Mater.* **48&45** (1990) 117.
9. R. MEHRABIAN, *Int. Met. Rev.* **27** (1982) 185.
10. Y.-W. KIM, W. M. GRIFFITH and F. H. FROES, *J. Metals* **32** (1985) 27.
11. M. A. ZAIDI, *Mat. Sci. Eng.* **98** (1988) 221.
12. D. J. SKINNER, M. S. ZEDALIS and P. GILMAN, *ibid.* **A119** (1989) 81.

Received 22 February
and accepted 1 December 1995